

# Functional Mechanism of the Abscisic Acid Agonist Pyrabactin\*<sup>§</sup>

Received for publication, May 27, 2010, and in revised form, June 6, 2010. Published, JBC Papers in Press, June 16, 2010, DOI 10.1074/jbc.M110.149005

Qi Hao<sup>‡§1</sup>, Ping Yin<sup>‡§1</sup>, Chuangye Yan<sup>‡¶1</sup>, Xiaoqiu Yuan<sup>‡§</sup>, Wenqi Li<sup>‡§</sup>, Zhiping Zhang<sup>||</sup>, Lei Liu<sup>||</sup>, Jiawei Wang<sup>‡¶</sup>, and Nieng Yan<sup>‡§2</sup>

From the <sup>‡</sup>State Key Laboratory of Biomembrane and Membrane Biotechnology, <sup>§</sup>Center for Structural Biology, School of Medicine, <sup>¶</sup>School of Life Sciences, and <sup>||</sup>Department of Chemistry, Tsinghua University, Beijing 100084, China

Pyrabactin is a synthetic abscisic acid (ABA) agonist that selectively inhibits seed germination. The use of pyrabactin was pivotal in the identification of the PYR1/PYL/RCAR family (PYL) of proteins as the ABA receptor. Although they both act through PYL proteins, pyrabactin and ABA share no apparent chemical or structural similarity. It remains unclear how pyrabactin functions as an ABA agonist. Here, we report the crystal structure of pyrabactin in complex with PYL1 at 2.4 Å resolution. Structural and biochemical analyses revealed that recognition of pyrabactin by the pocket residues precedes the closure of switch loop CL2. Structural comparison between pyrabactin- and ABA-bound PYL1 reveals a general principle in the arrangements of function groups of the two distinct ligands. The study provides a framework for the development of novel ABA agonists that may have applicable potentials in agriculture.

Abscisic acid (ABA)<sup>3</sup> is ubiquitous in higher plants, regulates a variety of processes during plant development, and protects plant against inclement environments such as cold and drought (1–3). PYR1/PYL/RCAR proteins (hereafter referred to as PYLs) were recently identified as a family of ABA receptors (4, 5). PYLs-mediated ABA signaling pathway was successfully recapitulated *in vitro* (6). In this pathway, transcription factors ABFs, which induce the expression of ABA-responsive genes, are activated through phosphorylation by SnRK2 kinases. The active, autophosphorylated SnRK2 kinases are subject to inhibition by the type 2C protein phosphatases (PP2Cs) such as ABI1, ABI2, and HAB1. PP2C-mediated negative regulation of ABA signaling is relieved by PYLs in an ABA-dependent manner (6, 7). Structural and biochemical studies elucidated the molecular mechanisms by which ABA-PYLs inhibit PP2Cs

(8–12). The apo-PYLs exist as a homodimer, with each protomer containing a ligand-binding pocket guarded by four conserved loops CL1–CL4 (9). Upon binding of a (+)-ABA molecule (hereafter referred to as ABA), the conserved loop CL2 undergoes a conformational switch and creates a novel binding surface (8–11). ABA binding also weakens the homodimeric interface of PYL (9). Consequently, ABA-bound PYL protein forms a 1:1 heterodimer with PP2C via the newly formed binding surface. CL2 of PYL proteins sits above the active site of PP2C and blocks substrate entry to PP2Cs, hence relieving PP2Cs-mediated inhibition of SnRK2 (9, 10, 12).

Chemical genetic analysis played an essential role in the identification of ABA receptors. Pyrabactin, an ABA-selective agonist and a synthetic inhibitor of seed germination (5, 13), was exploited for the isolation of pyrabactin resistance 1 (*Pyr1*) mutant alleles (5). PYR1, a representative member of PYL proteins, was shown to interact with PP2C in response to pyrabactin (5). Interestingly, although pyrabactin acts through PYL proteins, it shares no apparent chemical similarity with ABA (Fig. 1A). Thus, the available structural information fails to explain how pyrabactin agonizes ABA function.

Understanding the functional mechanism of pyrabactin will shed light on the development of novel ABA agonists that may have applicable potentials in agriculture. ABA is not a stable compound, and its costly synthesis further restricts its potential applications. Pyrabactin thus provides an alternative to the development of novel ABA-related compounds. In this paper, we performed biochemical and structural studies and report here the crystal structure of pyrabactin in complex with PYL1. Our study nicely illustrates how pyrabactin serves as an ABA agonist. Structural comparison with ABA-bound PYL1 revealed a general principle in the arrangement of function groups of the ligands.

## EXPERIMENTAL PROCEDURES

**Protein Preparation and Crystallization**—PYL1 (AT5G46790) and ABI1 (AT4G26080) were subcloned from the *Arabidopsis thaliana* cDNA library using standard PCR-based protocol. All mutants of PYL1 were generated with two-step PCR, verified by plasmid sequencing. All proteins were purified according the protocol described previously (9). Wild type and all mutants of PYL1 were expressed in *Escherichia coli* strain BL21(DE3) using vector pET-15b induced at 22 °C for 12 h. The individual proteins were purified with nickel-nitrilotriacetic acid resin (Qiagen), followed by anion-exchange chromatography (Source-15Q; GE Healthcare) and size-exclusion chromatography

\* This work was supported by Ministry of Science and Technology Grant 2009CB918802, Tsinghua University 985 Phase II funds, the Yuyuan Foundation, National Science Foundation of China Grant 20932006, and the Li Foundation.

<sup>§</sup> The on-line version of this article (available at <http://www.jbc.org>) contains supplemental Figs. 1–6.

The atomic coordinates and structure factors (codes 3NEF and 3NEG) have been deposited in the Protein Data Bank, Research Collaboratory for Structural Bioinformatics, Rutgers University, New Brunswick, NJ (<http://www.rcsb.org/>).

<sup>1</sup> These authors contributed equally to this work.

<sup>2</sup> To whom correspondence should be addressed: Rm. C329, Medical Science Bldg., Tsinghua University, Beijing 100084, China. Fax: 86-10-62792736; E-mail: nyan@tsinghua.edu.cn.

<sup>3</sup> The abbreviations used are: ABA, abscisic acid; PDB, Protein Data Bank; PP2C, protein phosphatase type 2C; PYR1, pyrabactin resistance 1; PYL, PYR1-like.

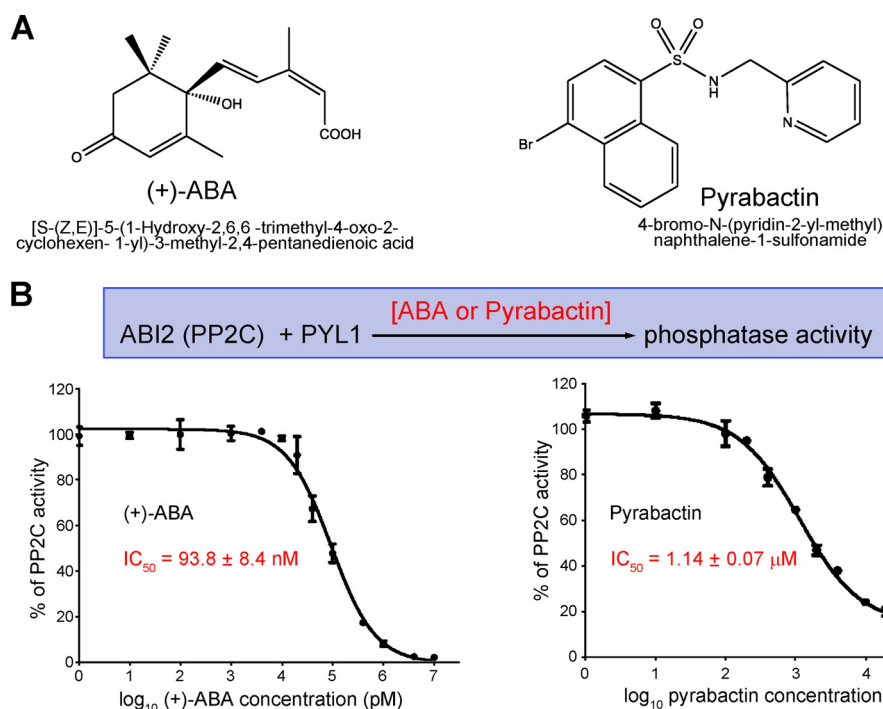


FIGURE 1. Inhibition of PP2C phosphatase activity by PYL1 in response to ABA and pyrabactin. *A*, chemical structures of (+)-ABA and pyrabactin. *B*, measurement of  $IC_{50}$  values of ABA and pyrabactin on ABI1 in the presence of PYL1. The phosphatase activity assay was conducted as previously described (9). The results are from three independent experiments, and error bars represent S.D.

**TABLE 1**  
Data collection and refinement statistics

	PYL1/PYB	PYL1/PYB
Data collection	Anisotropic data	High Resolution data
Space group	P3 <sub>1</sub> 21	P3 <sub>1</sub> 21
<b>Cell dimensions</b>		
<i>a</i> , <i>b</i> , <i>c</i> (Å)	130.23, 130.23, 88.25	128.57, 128.57, 87.24
$\alpha$ , $\beta$ , $\gamma$ (°)	90, 90, 120	90, 90, 120
Wavelength (Å)	0.92001	0.9067
Resolution (Å)	50~2.8 (2.95~2.8)	50~2.4 (2.53~2.4)
<i>R</i> <sub>merge</sub> (%)	9.5 (42.2)	10.3 (36.5)
<i>I</i> / $\sigma$ <i>I</i>	10.5 (3.4)	7.2 (2.6)
Completeness (%)	93.1 (54.5)	92.9 (54.8)
Redundancy	6.0	3.2
Resolution (Å)	50~2.8	50~2.4
No. reflections	8,331	30,549
<i>R</i> <sub>work</sub> / <i>R</i> <sub>free</sub> (%)	19.51/24.23	18.81/22.28
<b>No. atoms</b>		
Protein	2780	2870
Ligand/ion	45	22
Water	2	145
<b>B-factors</b>		
Protein	86.22	56.74
Ligand/ion	87.13	37.72
Water	71.91	49.73
<b>Root mean square deviations</b>		
Bond lengths (Å)	0.009	0.008
Bond angles (°)	1.312	1.248
<b>Ramachandran plot statistics (%)</b>		
Most favored	82.1	88.6
Additional allowed	17.3	9.9
Generously allowed	0.3	1.5
Disallowed	0.3	0.0

(Superdex-200; GE Healthcare). Prior to crystallization, PYL1 (residues 22–210) protein was incubated with pyrabactin with a molecular ratio of 1:2. Crystals were grown at 18 °C using the hanging-drop vapor diffusion method. Crystals appeared after 2 days in the well buffer containing 1.45 M Na/K tartrate, 100

mM Tris, pH 8.0, 1% octyl- $\beta$ -D-glucopyranoside (Anatrace), and 0.015% spermidine. Addition of 5.2 mM C<sub>8</sub>E<sub>5</sub> (Hampton Research) into the crystallization solution further improved the diffraction of the crystals.

**Data Collection, Structure Determination, and Refinement**—PYL1/PYB data were collected at the Shanghai Synchrotron Radiation Facility (SSRF) beamline BL17U and integrated with MOSFLM (14). Further processing was carried out using programs from the CCP4 suite (15). Data collection statistics are summarized in Table 1. PYL1 model (Protein Data Bank (PDB) code 3KDJ) was translated into the PYL1/PYB cell with the program PHASER (16) by the molecular replacement method. Manual model iterative rebuilding and refinement were performed with COOT (17) and PHENIX (18). The pyrabactin molecules were built into the cavity of the host protein molecules. Their

position and orientation were validated by the anomalous signal of bromide in the pyrabactin molecule.

**Phosphatase Activity Assay**—The phosphatase activity was measured by the Ser/Thr phosphatase assay system (Promega). Each reaction was performed in a 100- $\mu$ l reaction volume containing 1.8  $\mu$ g of ABI1, 1  $\mu$ g of wild type or mutant PYL1 proteins. 10  $\mu$ M ABA (Sigma-Aldrich) or pyrabactin was added when required. After incubation with peptide substrate (supplied with the Promega kit) in the buffer containing 50 mM imidazole, pH 7.2, 5 mM MgCl<sub>2</sub>, 0.2 mM EGTA, and 0.1 mg/ml bovine serum albumin at 30 °C for 15 min, the reaction was stopped by the addition of 100  $\mu$ l of molybdate dye and incubated for another 15 min at room temperature. Absorbance at 630 nm was measured. For the  $IC_{50}$  assay, the ligands were applied at the concentrations indicated in Fig. 1. The represented data are means  $\pm$  S.D. from three independent experiments.

## RESULTS

**Overall Structure of Pyrabactin-bound PYL1**—PYL1 inhibits PP2Cs phosphatase activity in an ABA-dependent manner. To examine whether PYL1 responds to pyrabactin similarly, we reconstituted a PP2C phosphatase activity assay *in vitro*. Consistent with the *in planta* observations (5), pyrabactin cannot directly inhibit the phosphatase activity of ABI1, but achieves the inhibition through PYL proteins (supplemental Fig. 1). Further characterization revealed that pyrabactin exhibits an  $IC_{50}$  (1.14  $\pm$  0.07  $\mu$ M)  $\sim$ 10-fold higher than that of ABA (93.8  $\pm$  8.4 nM) (Fig. 1*B*). We sought to understand the functional mechanism of pyrabactin by determining the crystal structure of pyrabactin-bound PYL1.

## Crystal Structure of PYL1 in Complex with Pyrabactin

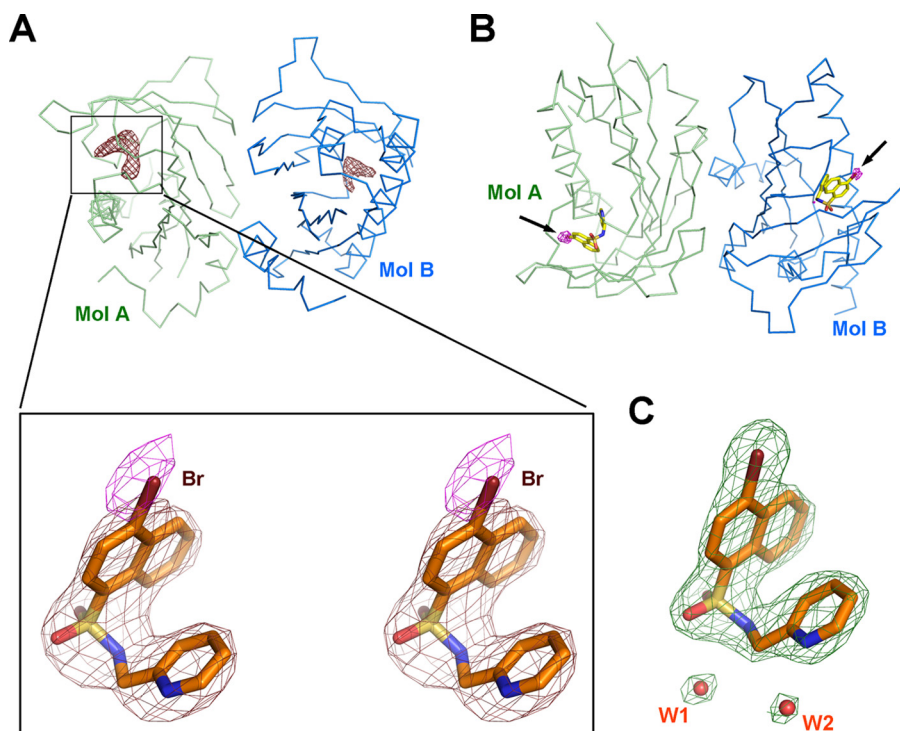


**FIGURE 2. Localization of pyrabactin molecules in the structure.** A, “omit” electron density maps for pyrabactin are shown. There are two PYL1 molecules (colored green and blue for Mol A and Mol B, respectively) in each asymmetric unit. The omit electron density map for pyrabactin in Mol A, shown in brown mesh, is contoured at  $3\sigma$ . A stereo view is shown in the inset. The position of the bromide atom is localized by the anomalous signal, shown in magenta mesh and contoured at  $3\sigma$ . B, anomalous signal of bromide facilitated the correct localization of pyrabactin in the pocket of PYL1. The diffraction data were collected at the peak wavelength of bromide. One major anomalous signal (magenta) was observed in the pocket of each PYL1 molecule. Pyrabactin molecules are shown as yellow sticks. C,  $2F_o - F_c$  electron density map of pyrabactin and two adjacent water molecules in Mol A in the 2.4 Å structure is shown. The map, shown in green mesh, is contoured at  $2\sigma$ . All structure figures were prepared with PyMOL.

In the presence of pyrabactin, PYL1 was crystallized in the space group  $P3_121$ . There are two protein molecules, named Mol A and Mol B, in each asymmetric unit (Fig. 2, A and B). The crystals diffracted anisotropically between 2.5 and 3 Å. The structure of PYL1 was determined by molecular replacement, and the final atomic model was refined to 2.8 Å resolution (Table 1 and supplemental Fig. 2). After all protein atoms were in place, a headset-shaped electron density appeared in the conserved pocket of each PYL1 molecule (Fig. 2A). This electron density allowed modeling of the pyrabactin molecule, and the position of the bromide atom in pyrabactin was confirmed by its anomalous signal (Fig. 2A and supplemental Fig. 3). Within the protein-ligand complex, pyrabactin adopts a U-shaped conformation. The pyridine and the naphthalene rings face each other with an angle of  $\sim 45$  degrees (supplemental Fig. 3B).

We next examined the two PYL1 molecules within each asymmetric unit. When Mol A and Mol B are superimposed, a prominent difference was observed in CL2 (supplemental Fig. 4A). Although CL2 in Mol A adopts a closed conformation, it remains open in Mol B even with pyrabactin binding. Pyrabactin binds to Mol A and Mol B in a similar manner, except for the lack of coordination by CL2 in Mol B (supplemental Fig. 4, A and B). This observation suggests that ligand binding into the pocket may precede the conformational change of CL2. Further examination of crystal packing revealed that Mol A exists as a monomer, whereas Mol B forms a homodimer with

the adjacent symmetry-related molecule (supplemental Fig. 4C). The structure of the dimeric pyrabactin-bound PYL1 (Mol B) is almost identical to that of apo-PYL1 (supplemental Fig. 4B), corroborating the hypothesis that dimer formation of PYLs may prevent conformational change of CL2 (9).

During the revision of this manuscript, we obtained the crystals of pyrabactin-bound PYL1 diffracting x-ray to 2.1 Å, when an additive, the detergent  $C_8E_5$ , was included in the crystallization solution. Due to the anisotropic diffraction ( $2.1 \text{ \AA} \times 2.5 \text{ \AA}$ ), the structure was refined to 2.4 Å resolution (Table 1). The high resolution structure is identical to the previous one, except that the anomalous signal of bromide was not detected in Mol B. The missing of the pyrabactin molecule in Mol B was probably due to the slightly modified crystallization condition. The electron density of pyrabactin and its surrounding waters in Mol A is of excellent quality (Fig. 2C and supplemental Fig. 5), so we therefore focus on Mol A for the analysis of the interaction between pyrabactin and PYL1.

**Recognition of Pyrabactin by PYL1**—The U-shaped pyrabactin sits in the conserved ligand-binding pocket of PYL1 with the bromonaphthalene ring positioned in proximity to CL2, while the pyridine group is away from the loop region and buried deep into the pocket (Fig. 3A). The coordination of pyrabactin is mediated by both polar and van der Waals contacts. Charged residues from CL1,  $\beta 3$ ,  $\beta 4$ , and  $\beta 7$  play an important role in coordinating pyrabactin via hydrogen bonds (Fig. 3B). The carboxylate of Glu<sup>121</sup> in strand  $\beta 4$  interacts with the sulfonamide of pyrabactin with both direct and water-mediated hydrogen bonds. Notably, a water molecule plays an important role in organizing the polar contacts between pyrabactin and PYL1. It accepts hydrogen bonds from the side chains of Lys<sup>86</sup> in CL1 and Arg<sup>106</sup> in strand  $\beta 3$  and the amine group of pyrabactin; meanwhile, it donates hydrogen bonds to the carboxylate of Glu<sup>121</sup> and the sulfone group of pyrabactin. The existence and the position of the pyridyl nitrogen were found essential for pyrabactin agonistic activity (5). The current structure showed that the pyridyl nitrogen is coordinated by the amine group of Lys<sup>86</sup> in CL1 and the carboxylate group of Glu<sup>171</sup> in  $\beta 7$  through water-mediated hydrogen bonds, supporting its essential role in mediating the ligand-protein interaction (Fig. 3B).

In contrast to the central portion of the U-shaped pyrabactin, the two arms of the ligand are relatively hydrophobic. They are buried in a hydrophobic environment surrounded by amino

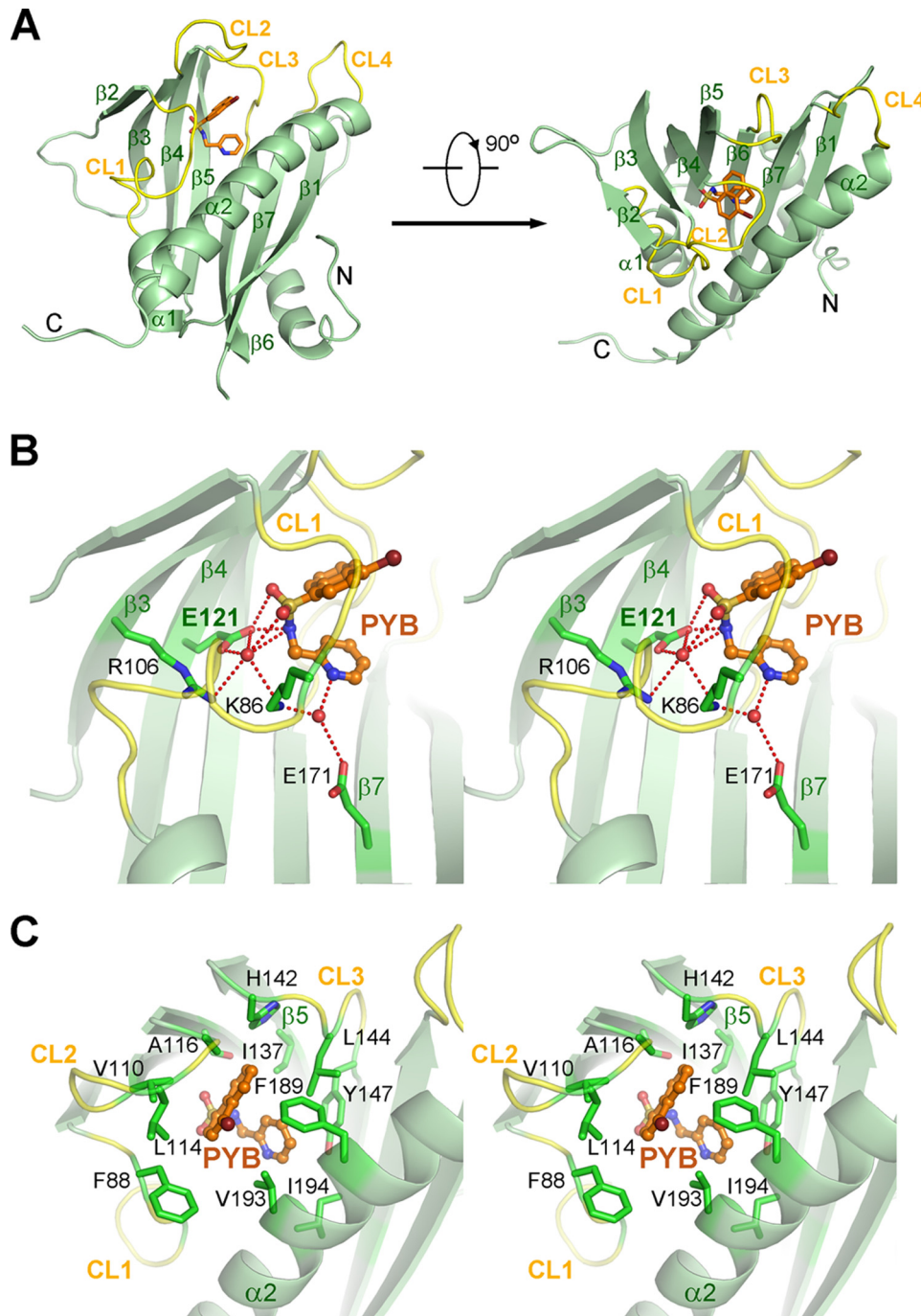


FIGURE 3. **Recognition of pyrabactin by PYL1.** A, overall structure of pyrabactin-bound PYL1. PYL1 is shown in green schematic, with the four conserved PYL loops, CL1–4, highlighted in yellow. Pyrabactin is displayed as orange sticks. B, pyrabactin recognition by PYL1 through polar interactions. The hydrogen bonds are highlighted in red, dashed lines. Two water molecules are shown as red spheres. A stereoview is shown. C, pyrabactin recognition by PYL1 through van der Waals contacts. The backbone of the protein is shown as a semitransparent diagram. A stereoview is shown.

acids mainly from CL1, CL2, CL3, and  $\alpha 2$ , which include Phe<sup>88</sup> in CL1; Val<sup>110</sup>, Leu<sup>114</sup>, and Ala<sup>116</sup> in CL2; His<sup>142</sup>, Leu<sup>144</sup>, and Tyr<sup>147</sup> in CL3; and Phe<sup>189</sup>, Val<sup>193</sup>, and Ile<sup>194</sup> in  $\alpha 2$  (Fig. 3C). Note that the geometric plate of CL2 is nearly in parallel with the hydrophobic naphthalene ring of pyrabactin. In particular, the bromide of pyrabactin is in close proximity to Val<sup>110</sup> and Leu<sup>114</sup> of CL2 (supplemental Fig. 5), indicating an important role of the bromide in rendering the closure of CL2.

**General Principle in Geometric Arrangement of Function Groups in Ligands**—At first glance, the coordination of pyrabactin by PYL1 seems to be different from that of ABA. However, when we superimposed the structure of pyrabactin-bound PYL1 on that of the ABA-bound PYL1, pyrabactin and ABA molecules overlap with each other, and the switch loop CL2 of PYL1 adopts a similar conformation (Fig. 4A). Notably, despite the distinct chemical structures, the spatial geometry of the function groups in pyrabactin and ABA is surprisingly similar to each other (Fig. 4B).

Both ligands are amphipathic, each comprising two polar modules buried deep inside the pocket and two hydrophobic modules adjacent to the switch loops (Fig. 4, A and B). The two hydrophobic modules of pyrabactin and ABA can be superimposed on each other. The primary hydrophobic module 1' comprises the 2,6,6-trimethyl-cyclohexene ring of ABA or the bromonaphthalene ring of pyrabactin. These two rings have a similar dimension of  $\sim 5 \text{ \AA} \times 5 \text{ \AA}$  (Fig. 4B, right panel). They may be the major driving force to pull the hydrophobic residues of CL2 over to achieve a closed conformation (Fig. 4A). A secondary hydrophobic module 2' comprises the methyl group in ABA and the pyridine ring of pyrabactin. This site is coordinated by hydrophobic residues from CL3 and helix  $\alpha 2$ . It may help anchor the ligands in the pocket (Figs. 3C and 4B).

In ABA, the two polar modules, the carboxylate and the hydroxyl groups, point into the conserved pocket and are coordinated mainly through water-mediated hydrogen bonds with charged or polar residues of PYL proteins (8–12). The two polar portions of pyrabactin, the pyridyl nitrogen and the sulfonamide group, adopt the same orientation. A closer examination revealed that the distance between the corresponding polar module 1 in ABA and pyrabactin, namely the carboxylate oxygen of ABA and the pyridyl nitrogen of pyrabactin, is 2.2  $\text{\AA}$ , whereas those between the corresponding polar module 2, the hydroxyl group of ABA and the amine-sulfone groups of pyrabactin, are 2.5  $\text{\AA}$ , 2.7  $\text{\AA}$ , and 2.9  $\text{\AA}$ , respectively. These distances are close to the length of hydro-

## Crystal Structure of PYL1 in Complex with Pyrabactin

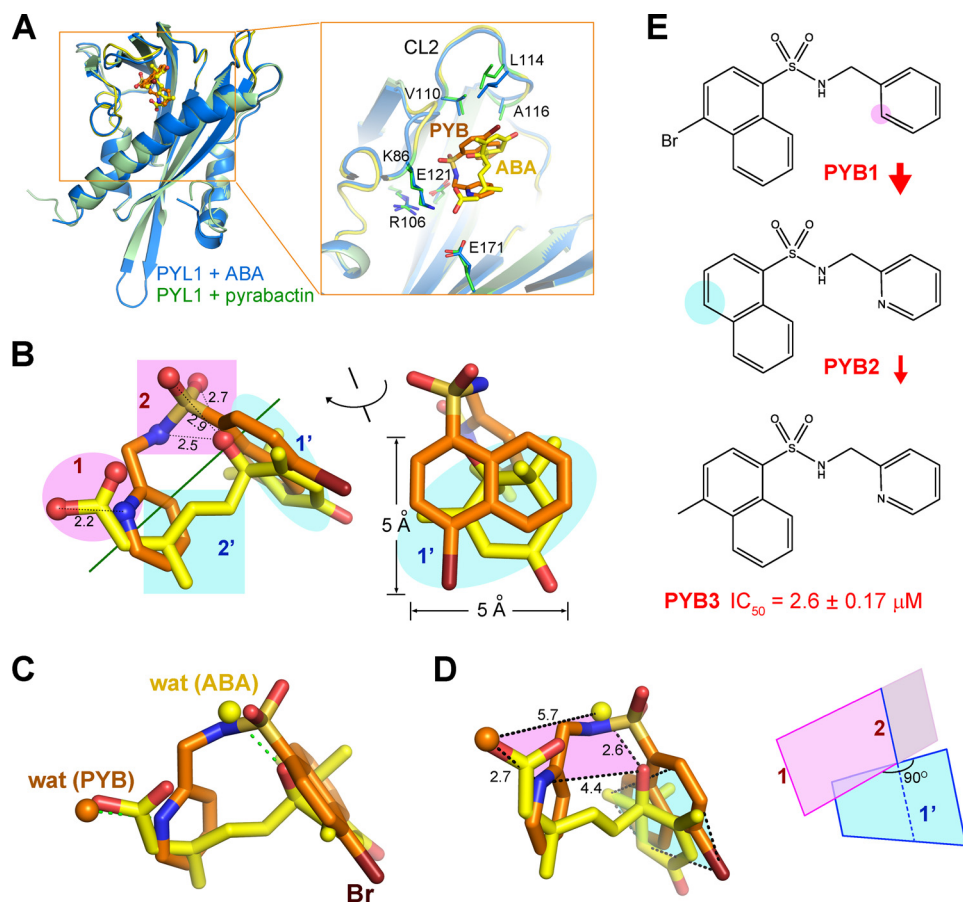


**FIGURE 4. General principle in the geometric arrangement of function groups of pyrabactin and ABA.** *A*, ABA and pyrabactin overlapped in the superimposed PYL1 structures. ABA and pyrabactin are shown as yellow and orange ball-and-sticks. The structure of ABA-bound PYL1 is from the ABA·PYL1·ABI1 ternary complex (PDB code 3KDJ). *Inset*, enlarged view of the superimposed ABA and pyrabactin molecules surrounded by key residues of PYL1. Four charged residues in the pocket and three hydrophobic residues of CL2, which play an important role in mediating the interaction between the ligands and the receptor, are shown as sticks. *B*, modular similarity between the structures of ABA and pyrabactin. The structures of ABA-bound and pyrabactin-bound PYL1 are superimposed as shown in *A*. Only the ligands are shown here. The two polar modules are highlighted in pink and annotated by 1 and 2. The two hydrophobic modules are highlighted in cyan and annotated by 1' and 2'. Two approximately perpendicular views are shown. Pyrabactin and ABA are shown in orange and yellow. The distances are measured in angstroms. The green line depicts the division of the polar and hydrophobic modules. *C*, water molecules exploited to compensate for the missing polar groups of either ligand for hydrophilic interaction with PYL1. A water molecule (yellow sphere) from the structure of ABA-bound PYL1 is located in the same position of the amine group of pyrabactin; likewise, a water molecule (orange sphere) from the structure of pyrabactin-bound PYL1 occupies the position of the carboxylate of ABA. *D*, geometric diagram of the ligands. The hydrophobic and the polar modules of the ligands are located in two perpendicular but not crossed plates. *E*, chemical characterization of the key function groups of pyrabactin. The red arrows beside the labels PYB1 and PYB2 indicate the compromised effects of the compounds on PYL1.

gen bond. Indeed, a water molecule, which mediates the interaction between the pyridyl nitrogen of pyrabactin and Lys<sup>86</sup> and Glu<sup>171</sup> of PYL1 (Fig. 2*B*), is located at the same position as the carboxylate oxygen atom in ABA, which directly contacts Lys<sup>86</sup> (Fig. 4, *A* and *C*) (8–12). Similarly, a water molecule that mediates the interaction between the hydroxyl group of ABA and Glu<sup>121</sup> of PYL1 is overlapped with the amine group of pyrabactin, which directly forms hydrogen bond with Glu<sup>121</sup> of PYL1 (Figs. 2*B* and 4*C*). The two water molecules compensate for the lack of the corresponding function groups in either ligand to complete the polar modules (Fig. 4*C*). Note that the two polar modules can be roughly aligned within the same plate which is almost perpendicular to the plate of hydrophobic module 1' (Fig. 4*D*). This arrangement may suggest a general principle in the design of novel ABA agonists which will be discussed later.

with that of ABA. Thus, modification of the function groups may result in varied efficacies of the ligands. In addition, water molecules play an important role in mediating the interaction between the ligands and the receptor. If a compound contains extended polar groups that occupy where the waters are localized, it may exhibit an increased binding affinity with the receptor because of the direct polar contacts.

*“Electromagnet” Model for Ligand Perception of PYL Proteins*—With the similar geometric arrangements of the function groups of pyrabactin and ABA, it is not surprising to see that the residues coordinating pyrabactin are almost identical to those involved in ABA recognition. These residues are mostly conserved in the PYL family of proteins (Fig. 5*A* and supplemental Fig. 5). We examined whether all of the four charged residues, Lys<sup>86</sup>, Arg<sup>106</sup>, Glu<sup>121</sup>, and Glu<sup>171</sup>, are essential in the ligand

The analyses also explained why the position of the pyridyl nitrogen is essential for pyrabactin function (5). If the nitrogen is located at any other sites on the pyridyl ring, it will be out of reach of the polar residues in PYL1 even in the presence of water molecules. In addition, an amine group on any other positions of the pyridyl ring would interfere with the hydrophobic module 2', which might be unfavorable to the hydrophobic environment within the receptor (Figs. 3*C* and 4*B*). To corroborate the analyses, we synthesized a few unreported variants of pyrabactin and examined their function. Removal of the pyridyl nitrogen (PYB1) or the bromide (PYB2) severely crippled the effect of the compounds on PYL1, whereas replacement of the bromide with a methyl group (PYB3) retains its function (Fig. 4*E*). PYL1 responds to PYB3 with an IC<sub>50</sub> of 2.6 ± 0.17 μM, comparable with that of pyrabactin. This observation indicates that a bulkier hydrophobic plate is required at hydrophobic module 1' so as to attract the CL2 switch to bend over (Fig. 4*D*).

It is noteworthy that there is no salt bridge mediating the interaction between pyrabactin and PYL1, whereas the salt bridge between the carboxylate of ABA and the amine group of the conserved Lys<sup>86</sup> in PYL1 is essential for ABA binding (9). This variation may partially account for the lower efficacy of pyrabactin in the PYL1-mediated PP2C inhibition compared

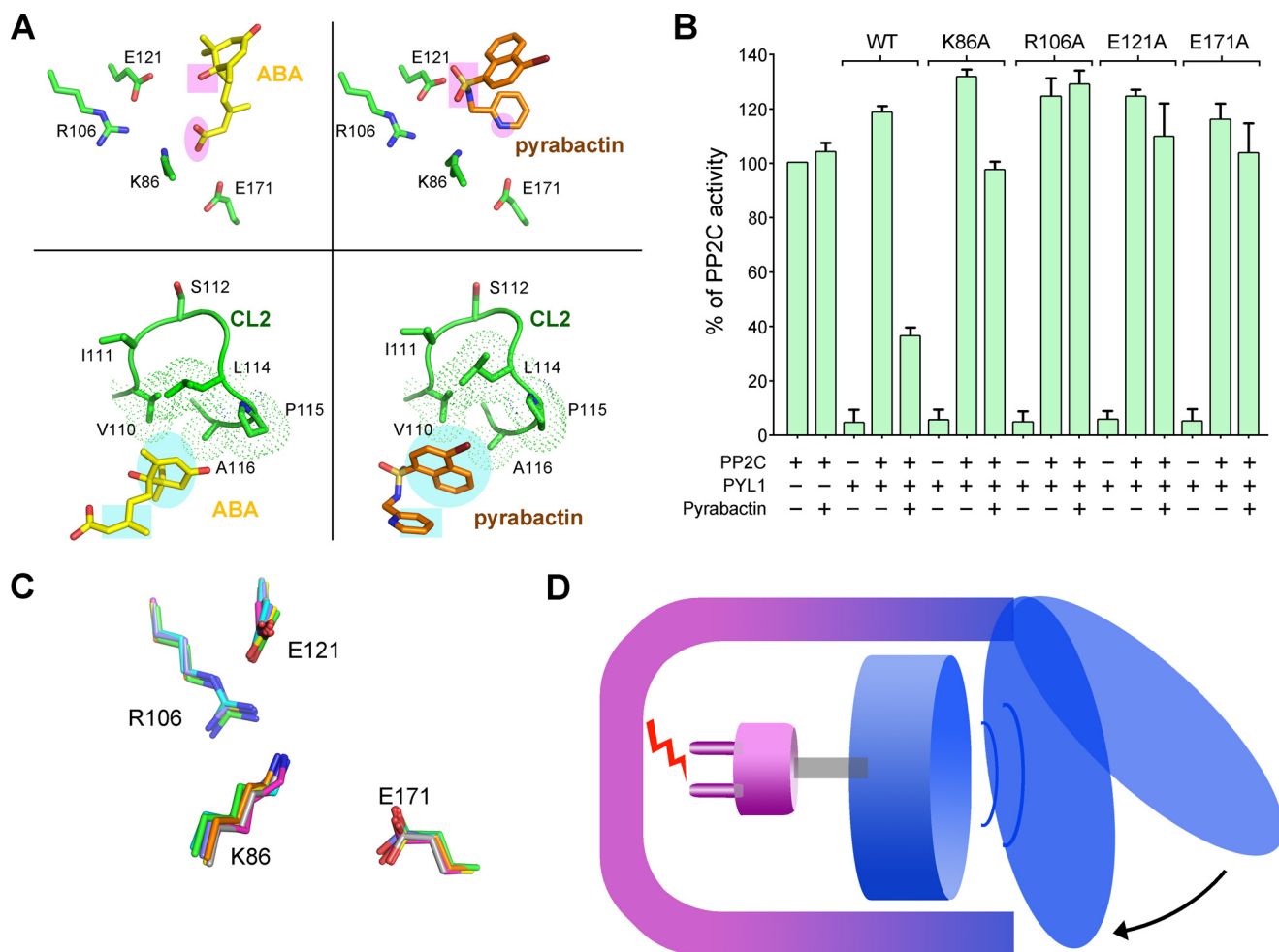


**FIGURE 5. Electromagnet model for ligand perception of PYL proteins.** *A*, conformation similarities of key residues involved in ligand binding in the structures of pyrabactin-bound and ABA-bound PYL1. *Upper panels*, charged residues of PYL1 that coordinate the polar modules of the ligands. *Lower panels*, hydrophobic residues in CL2 that are attracted by the hydrophobic module of the ligands. *B*, all four charged residues essential for PYL1 to respond to pyrabactin. The assay was performed independently at least three times; *error bars* represent S.D. *C*, identical conformations of the four charged residues in all available structures of PYL family proteins. The PDB codes for apo- and ABA-bound PYL1, and apo- and ABA-bound PYL2 are 3KAY, 3KDJ, 3KDH, and 3KDI. The PDB code for apo- and ABA-bound PYR1 is 3K3K. The seven structures are superimposed with PyMOL. *D*, schematic of electromagnet model that illustrates the ligand perception by PYL proteins. Refer to "Results" for detailed description.

binding. Single missense mutation of Lys<sup>86</sup>, Arg<sup>106</sup>, Glu<sup>121</sup>, and Glu<sup>171</sup> to Ala all rendered PYL1 insensitive to pyrabactin (Fig. 5B). These observations highlighted the essential roles of these highly conserved, charged residues of PYL proteins in ligand coordination. This result also suggests that neither of the polar modules of the ligands is dispensable for the ligand-receptor interaction. It thus further explains why the existence and the position of the pyridyl nitrogen are pivotal for the function of pyrabactin.

From the structural comparison we noticed that the four charged residues adopt identical conformations in ABA-bound and pyrabactin-bound PYL1. Are these conformations induced upon ligand binding or are they preexisting? To address this question, we superimposed all of the available structures of PYL proteins, including PYR1 and PYL2, in both apo- and ABA-bound forms, and PYL1 in apo-, ABA-bound, and pyrabactin-bound forms. In all seven structures, the four residues are arranged in an identical way (Fig. 5C), indicating a preexisting and rigid polar environment, in contrast to the induced hydrophobic portion exemplified by CL2. This facet should be taken

into account in the future design of ABA agonists targeting PYL proteins.

The observations suggest an electromagnet model for the ligand perception of PYL proteins. The polar modules of the ligands function like plugs. Once the polar plug is correctly anchored to the preexisting polar socket, the hydrophobic module of the ligand subsequently attracts the switch loop of PYLs to achieve a closed conformation as well as creating a PP2C-binding surface (Fig. 5D).

## DISCUSSION

Structural analyses of ABA-bound and pyrabactin-bound PYL1 revealed a general principle in designing ABA agonists that target PYL proteins (Fig. 4D). The ligand should be amphipathic with four modules: two polar modules positioned on one plate at one side of the compound; and at the other side a planar, bulky, hydrophobic module perpendicular to, but not crossed with, the polar modules. The polar modules are the anchor to be recognized by the hydrophilic pocket residues of

## Crystal Structure of PYL1 in Complex with Pyrabactin

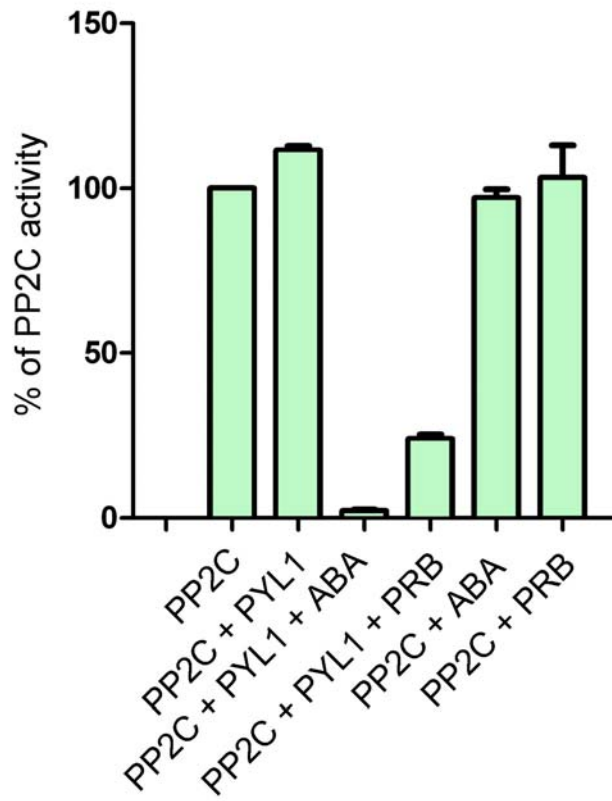
PYLs, whereas the hydrophobic module is responsible for the structural rearrangement of CL2.

In summary, our study reveals the molecular basis of pyrabactin agonistic activity on the ABA signaling pathway and provides a framework to develop novel ABA-related compounds for potential application in agriculture. However, it is known that pyrabactin is a selective agonist of ABA. It has a strong effect on PYR1, PYL1, etc., but has little or no effect on PYL2 and PYL4. Sequence alignment revealed that the residues involved in the coordination of pyrabactin are conserved among most of the 14 members of PYLs (supplemental Fig. 6). The current study and the available structural information cannot provide an explanation to the selectivity of pyrabactin by PYL proteins. Nonetheless, the existence of the “closed” monomer (Mol A) and the “open” dimer (Mol B) of PYL1 in the crystal structure provides a clue to address this question. It is possible that pyrabactin may be able to bind to other PYLs but unable to induce the closure of CL2 in PYL2 or PYL4 if these PYLs have a tighter dimer formation so as to effectively prevent the conformational change of CL2. The answer to this question may require additional structures of PYL proteins in complex with pyrabactin as well as associated computational, biochemical, and biophysical analyses.

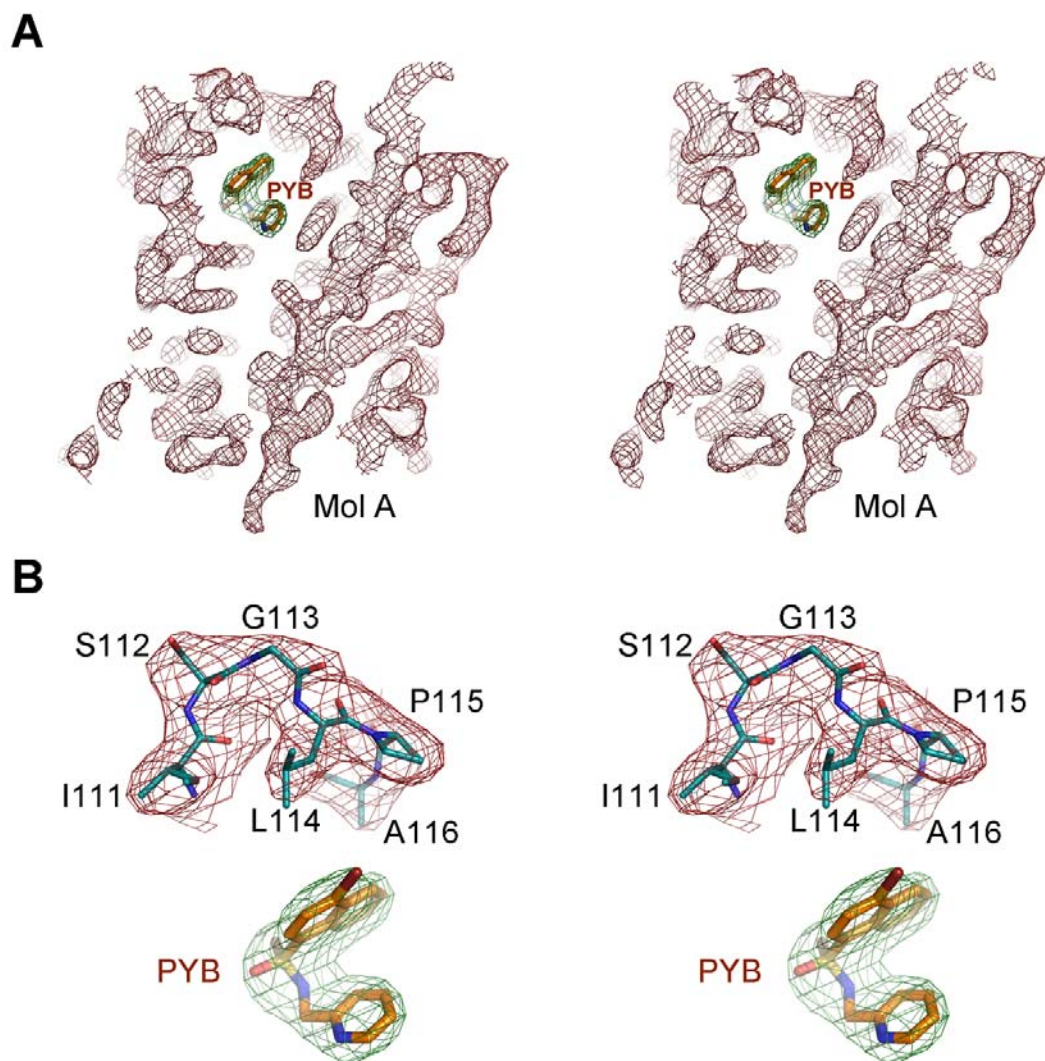
*Acknowledgments*—We thank J. He and S. Huang at the Shanghai Synchrotron Radiation Facility.

### REFERENCES

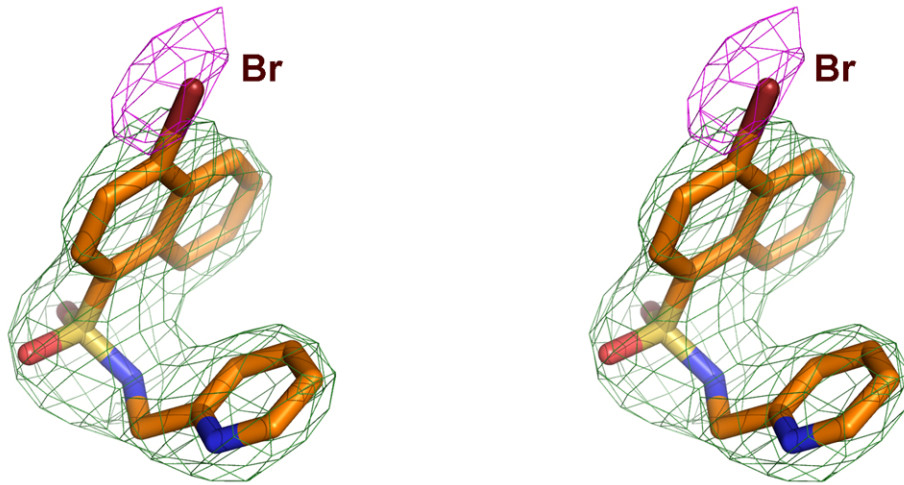
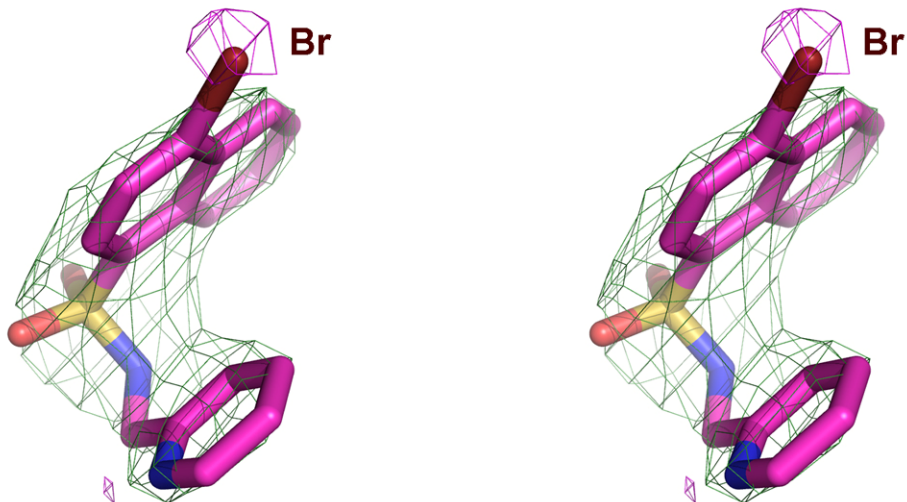
1. Fedoroff, N. V. (2002) *Sci. STKE* **2002**, re10
2. Finkelstein, R., Reeves, W., Ariizumi, T., and Steber, C. (2008) *Annu. Rev. Plant Biol.* **59**, 387–415
3. Schroeder, J. I., and Nambara, E. (2006) *Cell* **126**, 1023–1025
4. Ma, Y., Szostkiewicz, I., Korte, A., Moes, D., Yang, Y., Christmann, A., and Grill, E. (2009) *Science* **324**, 1064–1068
5. Park, S. Y., Fung, P., Nishimura, N., Jensen, D. R., Fujii, H., Zhao, Y., Lumba, S., Santiago, J., Rodrigues, A., Chow, T. F., Alfred, S. E., Bonetta, D., Finkelstein, R., Provart, N. J., Desveaux, D., Rodriguez, P. L., McCourt, P., Zhu, J. K., Schroeder, J. I., Volkman, B. F., and Cutler, S. R. (2009) *Science* **324**, 1068–1071
6. Fujii, H., Chinnusamy, V., Rodrigues, A., Rubio, S., Antoni, R., Park, S. Y., Cutler, S. R., Sheen, J., Rodriguez, P. L., and Zhu, J. K. (2009) *Nature* **462**, 660–664
7. Cutler, S. R., Rodriguez, P. L., Finkelstein, R. R., and Abrams, S. R. (2010) *Annu. Rev. Plant Biol.* **61**, 26.21–26.29
8. Nishimura, N., Hitomi, K., Arvai, A. S., Rambo, R. P., Hitomi, C., Cutler, S. R., Schroeder, J. I., and Getzoff, E. D. (2009) *Science* **326**, 1373–1379
9. Yin, P., Fan, H., Hao, Q., Yuan, X., Wu, D., Pang, Y., Yan, C., Li, W., Wang, J., and Yan, N. (2009) *Nat. Struct. Mol. Biol.* **16**, 1230–1236
10. Melcher, K., Ng, L. M., Zhou, X. E., Soon, F. F., Xu, Y., Suino-Powell, K. M., Park, S. Y., Weiner, J. J., Fujii, H., Chinnusamy, V., Kovach, A., Li, J., Wang, Y., Li, J., Peterson, F. C., Jensen, D. R., Yong, E. L., Volkman, B. F., Cutler, S. R., Zhu, J. K., and Xu, H. E. (2009) *Nature* **462**, 602–608
11. Santiago, J., Dupeux, F., Round, A., Antoni, R., Park, S. Y., Jamin, M., Cutler, S. R., Rodriguez, P. L., and Márquez, J. A. (2009) *Nature* **462**, 665–668
12. Miyazono, K., Miyakawa, T., Sawano, Y., Kubota, K., Kang, H. J., Asano, A., Miyauchi, Y., Takahashi, M., Zhi, Y., Fujita, Y., Yoshida, T., Kodaira, K. S., Yamaguchi-Shinozaki, K., and Tanokura, M. (2009) *Nature* **462**, 609–614
13. Zhao, Y., Chow, T. F., Puckrin, R. S., Alfred, S. E., Korir, A. K., Larive, C. K., and Cutler, S. R. (2007) *Nat. Chem. Biol.* **3**, 716–721
14. Leslie, A. G. (1992) *Joint CCP4/ESF-EAMCB Newslett. Protein Crystallogr.* **26**
15. Collaborative Computational Project, No. 4 (1994) *Acta Crystallogr.* **D50**, 760–763
16. McCoy, A. J., Grosse-Kunstleve, R. W., Adams, P. D., Winn, M. D., Storoni, L. C., and Read, R. J. (2007) *J. Appl. Crystallogr.* **40**, 658–674
17. Emsley, P., and Cowtan, K. (2004) *Acta Crystallogr.* **60**, 2126–2132
18. Adams, P. D., Grosse-Kunstleve, R. W., Hung, L. W., Ioerger, T. R., McCoy, A. J., Moriarty, N. W., Read, R. J., Sacchettini, J. C., Sauter, N. K., and Terwilliger, T. C. (2002) *Acta Crystallogr.* **58**, 1948–1954



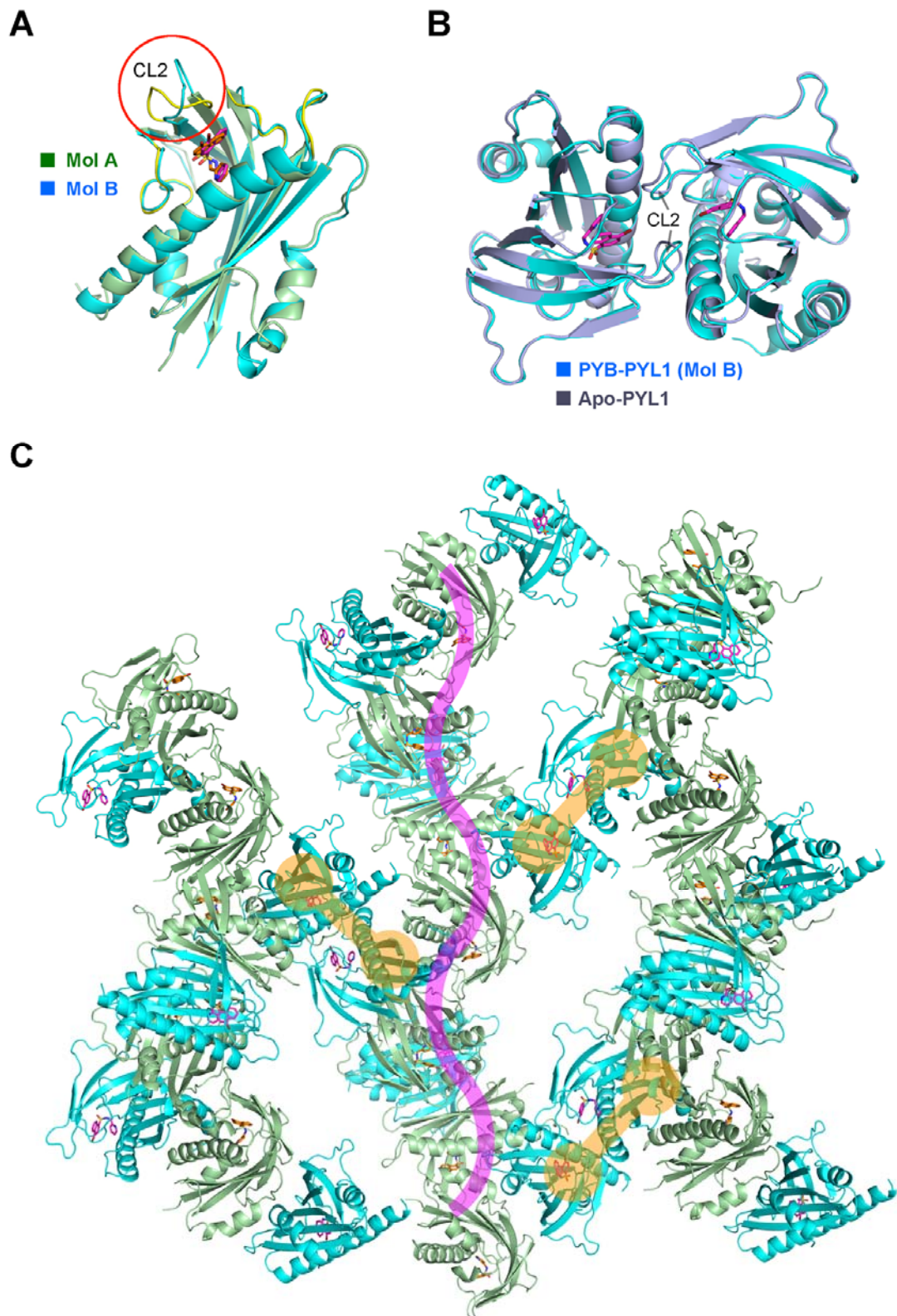
**Supplementary Figure 1.** Inhibition of PP2C by PYL1 in response to pyrabactin and ABA. PYL1 inhibits the phosphatase activity of ABI1 in response to both pyrabactin and ABA. Pyrabactin showed a lower inhibitory efficacy compared to ABA.



**Supplementary Figure 2.** The 2Fo-Fc electron density maps for pyrabactin-bound PYL1 (Mol A). (A) The 2Fo-Fc electron density map of pyrabactin-bound PYL1, shown in brown mesh for the protein and green mesh for the ligand, is contoured at  $1.0 \sigma$  and shown in stereo view. (B) A stereo view of the 2Fo-Fc electron density maps for CL2 and pyrabactin in Mol A.

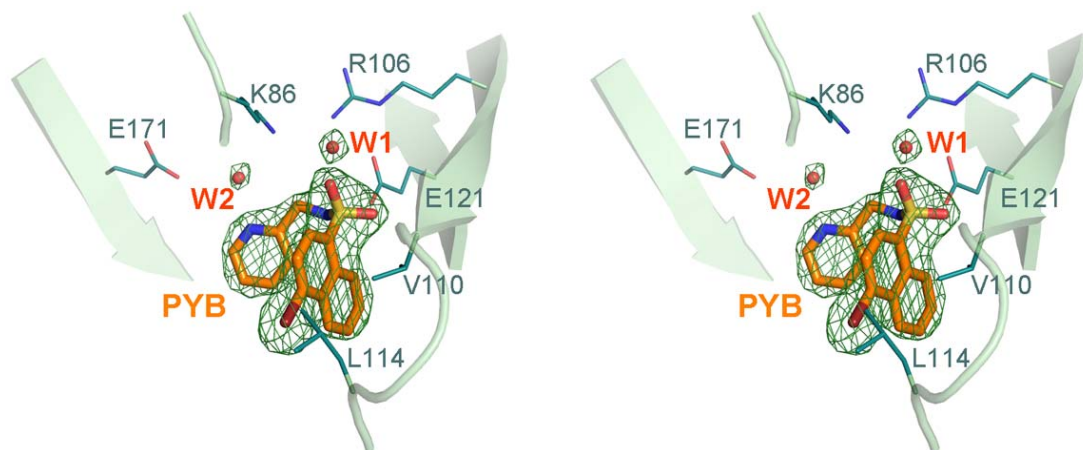
**A****B**

**Supplementary Figure 3.** The stereo view of 2Fo-Fc electron density maps for pyrabactin in Mol A (A) and Mol B (B), shown in green mesh and contoured at  $1\sigma$ , are displayed in the inset. The anomalous signal for bromide is shown in magenta mesh and contoured at  $3\sigma$ .

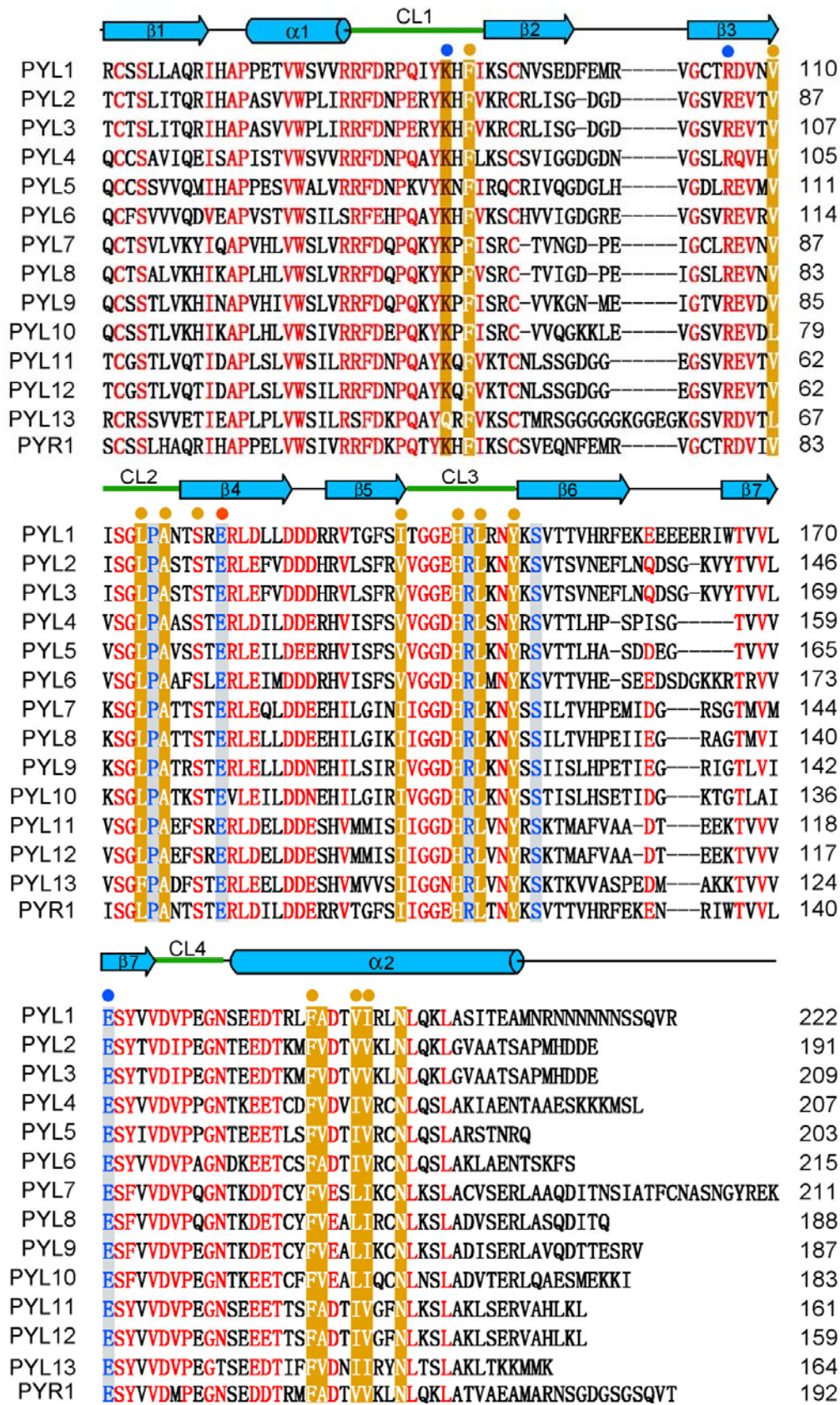


**Supplementary Figure 4** Mol A and Mol B of PYL1 exhibit distinct conformations in the switch loop CL2. (A) Mol A of PYL1 exhibits a closed conformation, whereas Mol B remains open. (B) The conformation of Mol B is similar to that of

apo-PYL1 despite of pyrabactin binding. (C) Crystal packing of pyrabactin-bound PYL1. The orange dumbbell indicates the dimer of Mol B formed by two adjacent symmetry-related molecules. By contrast, Mol A fails to form a dimer, but stacks against each other in a tandem way, as indicated by the magenta curve.



**Supplementary Figure 5** The stereoview of the 2Fo-Fc electron density map of pyrabactin (orange sticks) and two adjacent water molecules (red spheres) in Mol A in the 2.4 Å structure. The map, shown in green mesh, is contoured at  $2\sigma$ . Some of the key residues of PYL1 that are involved in pyrabactin recognition are shown in sticks.



**Supplementary Figure 6.** PYL1 coordinates pyrabactin and ABA with similar, conserved residues. PYL residues that are directly involved in ABA binding are colored white and highlighted in orange background. Residues that coordinate ABA through water molecules are colored blue, with grey background. The residue that forms direct hydrogen bonds with pyrabactin is indicated by the red dot. Residues that interact with pyrabactin through water-mediated hydrogen bonds and van der Waals interactions are indicated by blue and orange dots, respectively. Note that the residues that coordinate pyrabactin are almost identical to those that are involved in ABA binding and are highly conserved among the 14 PYL family members.

**Functional Mechanism of the Abscisic Acid Agonist Pyrabactin**  
Qi Hao, Ping Yin, Chuangye Yan, Xiaoqiu Yuan, Wenqi Li, Zhiping Zhang, Lei Liu,  
Jiawei Wang and Nieng Yan

*J. Biol. Chem.* 2010, 285:28946-28952.

doi: 10.1074/jbc.M110.149005 originally published online June 16, 2010

---

Access the most updated version of this article at doi: [10.1074/jbc.M110.149005](https://doi.org/10.1074/jbc.M110.149005)

Alerts:

- [When this article is cited](#)
- [When a correction for this article is posted](#)

[Click here](#) to choose from all of JBC's e-mail alerts

Supplemental material:

<http://www.jbc.org/content/suppl/2010/06/16/M110.149005.DC1.html>

This article cites 17 references, 4 of which can be accessed free at  
<http://www.jbc.org/content/285/37/28946.full.html#ref-list-1>